PROCEEDINGS OF SCIENCE

X(3872) and its bottomonium counterpart at ATLAS

K. Kordas*, **on behalf of the ATLAS Collaboration**
Department of Physics, Aristotle University of Thessaloniki, Thessaloniki, Greece
E-mail: Kostas.Kordas@cern.ch, kostaskordas@auth.gr

We present the measurement of the differential cross-section of the $X(3872)$ state through its decays to $J/\psi\pi^+\pi^-$ final state . The cross-section was extracted for both prompt and non-prompt production. The existence of the $X(3872)$ suggests the presence of its bottomonium counterpart X_b. Search for X_b with the ATLAS experiment in several final states, including $\Upsilon\pi^+\pi^-$, is presented.

XXIV International Workshop on Deep-Inelastic Scattering and Related Subjects
11-15 April, 2016
DESY Hamburg, Germany

*Speaker.

PoS(DIS2016)160

1. Brief status of X(3872)

The $X(3872)$ is the best-studied of the new hidden-charm states seen in the last decade, and heavy-quark symmetry suggests the existence of a hidden-beauty partner referred to as X_b, which should be produced in pp collisions. After reviewing briefly the status of $X(3872)$ here, the next Section presents a search for the X_b and other hidden-beauty states by ATLAS [1].

The $X(3872)$ was observed by Belle in decays $B^{\pm} \to K^{\pm}X(\to \pi^+\pi^- J/\psi)$ [2], and it was subsequently confirmed by others. CDF [3] and D$\emptyset$ [4] found that the $X(3872)$ is produced mostly directly in $p\bar{p}$ collisions; only $\simeq 16\%$ of $X(3872)$ is the result of B decays [3].

At the LHC, CMS has used the dataset of 4.8 fb^{-1} from 7 TeV pp collisions to measure the product of the $pp \to X(3872)$ production cross section times the branching fraction $X(3872) \to J/\psi\pi^+\pi^-$ to be $(6.56 \pm 0.29 \pm 0.65)\%$ of the similar production cross section times branching ratio product for $\psi(2S)$ decaying to $J/\psi\pi^+\pi^-$ [5]. No significant dependence on the p_T of the system was found; in addition, it is observed that the theory describes the shape of the diffential cross section reasonably well, but it overestimates the value by a factor of three [5].

ATLAS has released a detailed study of the reference channel $\psi(2S) \to J/\psi\pi^+\pi^-$ using 2.1 fb^{-1} of the 7 TeV dataset and found that the theory (NLO NRQCD) describes the absolute cross section and shape fairly well [6]. Furthermore, the fraction of non-prompt $\psi(2S)$ production is significant; it drops from $\sim 80\%$ to $\sim 20\%$ as the p_T increases, unlike the almost flat $\sim 26\%$ non-prompt fraction for the $X(3872)$ production seen by CMS [5].

Recently, LHCb determined unambiguisly the quantum numbers of $X(3872)$ to be $J^{PC} = 1^{++}$ [7]. The plethora of measuremenets about its mass, width, decay characteristics and quantun numbers, indicate that the $X(3872)$ is unlikely to be a conventional quarkonium ($c\bar{c}$) state. Various other models are proposed in the literature to describe its structure; from $[qc][\bar{q}\bar{c}]$ tetraquark models, to weakly bound $D^0\bar{D}^{\star 0}$ molecular models, with the later been popular due to the proximity of the $X(3872)$ mass to the $D^0\bar{D}^{\star 0}$ threshold. The definite LHCb observation of the decay $X(3872) \to \psi(2S)\gamma$ at a rate $\simeq 2.5$ times the $X(3872) \to J/\psi\gamma$ rate, suggests that the $X(3872)$ can not be a pure $D^0\bar{D^{\star 0}}$ "molecule" and it is probably a mixture of $D^0\bar{D}^{\star 0}$ and $c\bar{c}$ states [8].

2. Search for X_b in ATLAS

ATLAS searched for the X_b and other hidden-beauty states using the decay mode $\pi^+\pi^-\Upsilon(1S)$, with $\Upsilon(1S) \to \mu^+\mu^-$, which is analogous to the discovery mode of $X(3872)$; a data sample of pp collisions at $\sqrt{s} = 8$ TeV which was collected during the 2012 run of the LHC and amounts to an integrated lumonosity of 16.2 fb^{-1}, was used [9]. By analogy to $X(3872)$, the molecular model suggests a X_b mass close to $B\bar{B}^{(\star)}$, i.e. ~ 10.56 GeV.

The $\Upsilon(2S)$ and $\Upsilon(3S) \to \pi^+\pi^-\Upsilon(1S)$ peaks are used to validate the measurement technique, and search results are presented in terms of the product of the new particle's production cross section (σ) and its' branching fraction (B) to $\pi^+\pi^-\Upsilon(1S)$, relative to the equivalent quantity for the $\Upsilon(2S)$; this ratio, $(\sigma B)/(\sigma B)_{2S}$, is termed R.

Two oppositely charged muons with $p_T > 4$ GeV, $|\eta| < 2.3$ and a $\mu^+\mu^-$ mass within ± 350 MeV around the world average $\Upsilon(1S)$ mass [10], form the $\Upsilon(1S)$ candidates. These are combined with two oppositely charged tracks with $p_T > 400$ MeV and $|\eta| < 2.5$ which are assinged the

pion mass, and a four-track vertex is formed. The muon pair mass is constrained to the world average $\Upsilon(1S)$ mass to improve the $X_b \to \pi^+\pi - \Upsilon(1S)$ mass resolution; e.g., the RMS in the $\Upsilon(2S)$ simulation improves from 142 MeV to 9.7 MeV. After a χ^2 cut on the vertex fit quality to reduce background, all remaining $\pi^+\pi^-\Upsilon(1S)$ combinations with masses up to 11.2 GeV are retained as X_b candidates.

Three kinematic variables of the parent X_b candidate are used, each split in two regions, to define eight bins of varying signal sensitivity: first, the much better mass resolution in the barrel region of the detector, leads to separating the candidates among the barrel ($|y|$<1.2) and the endcap ($1.2 < |y| < 2.4$) regions; then, the transverse momentum is split in two regions, $p_T < 20$ GeV and $p_T > 20$ GeV; and last, the $cos\theta^\star$ can be positive or negative, where $\theta^\star$ is the angle between the $\pi^+\pi^-$ momentum in the parent rest frame and the parent momentum in Lab.

Simulation is used to derive the signal fraction in these eight bins. The fraction of signal in the low-value region of each kinematic variable is defined as "splitting function", S. Thus, $S_{|y|} = 0.606 \pm 0.004$, means that the signal in the barrel (|y|<1.2) region is 60.6% of all signal, integrating over p_T and $cos\theta^\star$; the fraction of events in the encap (1.2<|y|<2.4) is simply $1 - S_{|y|}$. Separately for the barrel and endcap regions, splitting functions $S^b_{p_T}$ and $S^{ec}_{p_T}$ are then defined for p_T, and then four splitting functions, $S^{(i)}_{cos\theta^\star}$, are defined for $cos\theta^\star$, where $i = 1-4$ respresents one of the four $\{|y|, p_T\}$ bins. The simulation indicates that the splitting function in $|y|$ is constant with the mass of the parent, while the other splitting functions depend on the mass and their functional dependence is derived from the simulation. Thus, the fraction of signal in each of the eight kinematical bins is calculated. E.g., the fraction of signal in the bin ($|y| < 1.2, p_T > 20$ GeV, $cos\theta^\star < 0$) is given by $S_{|y|} \cdot (1 - S^b_{p_T}(m)) \cdot S^{(3)}_{cos\theta^\star}(m)$.

On Figure 1 (left) the distribution of the $\pi^+\pi^-\Upsilon(1S)$ mass in the most sensistive bin is shown. Only the $\Upsilon(2S)$ and $\Upsilon(3S)$ peaks are visible. Binned extended maximum-likelihood fits in a local region around the $\Upsilon(2S)$ and $\Upsilon(3S)$ peaks, with a bin width of 2 MeV, are performed. The signal is fit with two Gaussians with a common mean, a narrow component fraction and a ratio of broad to narrow widths which are found to be independent of mass; in contrast, the narrow component width reflects the different detector resolution between barrel and encap and also varies as a function of mass. Thus, for each hypothesis on the parent mass, both the signal shape and the signal fraction have a well modeled dependancy on the parent mass. The background is described by a linear combination of Chebychev polynomials up to second-order. On Figure 1 (right), the measured $\Upsilon(2S)$ invariant mass (data points), together with fits (solid curves) to the $\Upsilon(2S)$ peak in the barrel is shown, with signal mass (m) and width (σ_b) parameters free; these are found consistent with those fitted in simulated $\Upsilon(2S)$ events. Comparison of the $\Upsilon(2S)$ and $\Upsilon(3S)$ signals and their yields between data and simulation are used to calibrate the simulation predictions on the splitting functions and the event yields for the X_b search.

In searching for the X_b, a hypothesis test for its presence is performed in the $\pi^+\pi^-\Upsilon(1S)$ mass distribution, from 10 to 11 GeV in steps of 10 MeV, assuming a narrow state with a differential cross section in (|y|,p_T) similar to that of $\Upsilon(2S)$ or $\Upsilon(3S)$. Excluding the $\Upsilon(2S)$ and $\Upsilon(3S)$ regions, the tested masses are in the ranges $10.05 - 10.31$ and $10.40 - 11.00$ GeV. At each mass hypothesis, all eight signal bins are fit simultaneously, using the same maximum likelihood fit as for the $\Upsilon(2S)$ and $\Upsilon(3S)$ cases above, and a p-value is extracted using the asymptotic formula for the $q0$ statistic

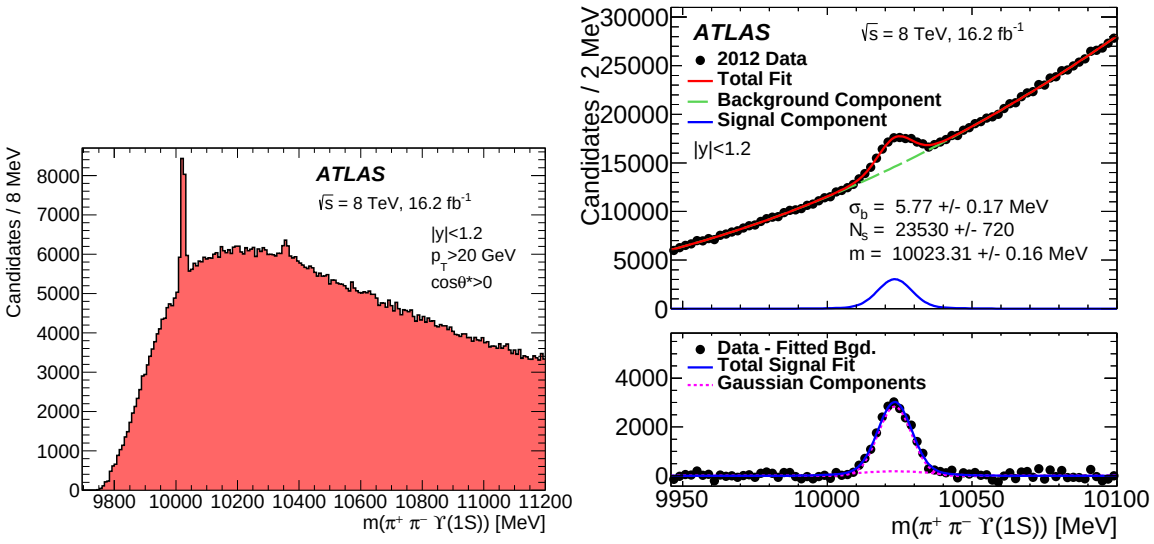

Figure 1: Left: The $\pi^+\pi^-\Upsilon(1S)$ invariant mass distribution in the kinematic bin most sensitive to an X_b signal: $|y| < 1.2, p_T > 20$ GeV, and $cos\theta^\star > 0$. The only apparent peaks are at the masses of the $\Upsilon(2S)$ (10023 MeV) and $\Upsilon(3S)$ (10355 MeV). Right: the measured $\Upsilon(2S)$ invariant mass (data points), together with fits (solid curves) to the $\Upsilon(2S)$ peak in the barrel is shown, with signal mass (m) and width (σ_b) parameters free; the lower panel shows background-subtracted data, with the total signal function (solid) and its two Gaussian components (short-dashed curves) overlaid. Figures taken from Ref. [9].

[11], which is a modification of the standard likelihood ratio. No evidence for new states with local significance more than 3 is found (see left side of Figure 2).

The expected yield of X_b can be extrapolated from the N_{2S} yield, using the X_b production rate (σB, its production cross section multiplied by its branching fraction to $\pi^+\pi^-\Upsilon(1S)$) relative to that of the $\Upsilon(2S)$, $R = (\sigma B)/(\sigma B)_{2S}$. The simulation is used to calculate the needed relative acceptances and efficinecies of X_b with repsect to those of $\Upsilon(2S)$. Thus, expected p-values can be extracted, as seen on the left side of Fig. 2, where $R = 6.56\%$ (the value for the production of $X(3872)$ relative to $\psi(2S)$ [5]), and $R = 3\%$, are used for demonstration.

Since no evidence for new states is found, upper limits on the relative production rate, R, are evaluated at the 95% confidence level using the CL_S method, by implementing asymptotic formulae for the $\tilde{q_\mu}$ statistic [11]. The results (right side of Figure 2, solid line) range between $R = 0.8\%$ and 4.0%. Median expected upper limits assuming background only (dashed line), and corresponding $\pm 1\sigma$ and $\pm 2\sigma$ bands are also shown.

These limits include the effect of systematic uncertainties on the nuisance parameters entering the upper limit calculation, with the following two being the dominante ones: i) in the X_b decay to $\pi^+\pi^-\Upsilon(1S)$, the three-body phase space was used as a default, but $\Upsilon(2S)$ and $\Upsilon(3S)$-like distributions of the decay products change the splitting functions by up to 35%, decrease the efficiency ratio by up to 17%, and produce modest changes in other parameters; ii) the ratio of acceptances of an X_b of a given mass w.r.t the $\Upsilon(2S)$ is taken by a linear extrapolation from the $\Upsilon(2S)$ to the $\Upsilon(3S)$ masses, but alternative extrapolations between the $\Upsilon(1S)$ and $\Upsilon(2S)$, and between $\Upsilon(1S)$ and $\Upsilon(3S)$, are also tried, and can change the acceptance ratio up to 12%, which is assigned as the uncertainty.

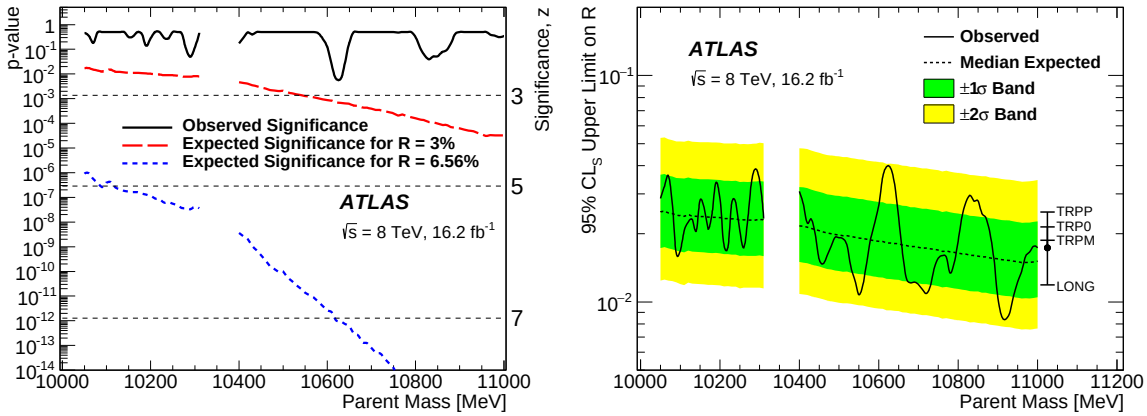

Figure 2: Left: The solid curve shows the observed local p-value for the background-only hypothesis (left scale), and the corresponding significance, z, of a peak in $\pi^+\pi^-\Upsilon(1S)$ (right scale), as a function of the mass of a hypothetical X_b parent state. Also shown are the expected p-values for the case of a signal with R=3% (long-dashed line) and R=6.56% (dashed curve). Right: Observed 95%CL_S upper limits (solid line) on the relative production rate R of a hypothetical X_b parent state decaying isotropically to $\pi^+\pi^-\Upsilon(1S)$, as a function of mass. The median expectation (dashed) and the corresponding $\pm1\sigma$ and $\pm2\sigma$ bands are also shown. The bar on the right shows typical shifts under alternative X_b spin-alignment scenarios, relative to the isotropic ("FLAT") case shown with the solid point. Figures taken from Ref. [9].

Systematic effects are added in quadrature, and their inclusion increases the observed limits by up to 13% and inflate the $\pm1\sigma$ band by $9.5\% - 25\%$, depending on the X_b mass (see Figure 2, right). The effect of the X_b spin-alignment model is not taken as systematic, but is shown separately. The X_b spin-alignment is unknown and is taken to be unpolarised ("FLAT"), but since this can have a strong impact on the upper limit, the limits are re-derived under longitudinal ("LONG") and three transverse ("TRPP", "TRP0", "TRPM") spin-alignment scenarios [12]. Shifts in the upper limits have a weak dependence on mass and so in Fig. 2 the effect of each spin-alignment hypothesis is represented by a single number: the difference in the median expected CL_S from the "FLAT" case.

Within the same analysis framework, searches for the $\Upsilon(1^3D_J)$ triplet and for the broad states $\Upsilon(10860)$ and $\Upsilon(11020)$ were performed. For $\Upsilon(1^3D_J)$ two extra peaks were added to the signal model. Masses 10156, 10164 and 10170 MeV were assumed (indicated by the previously measured mass for the $\Upsilon(1^D_2)$ [10] and the triplet mass splitting expected in the literature). Assuming independent normalisations but common signal shapes and split functions, no evidence of the triplet is found, with various mass splittings tried. If the $\Upsilon(1^3D_2)$ dominates the triplet or its mass splitting is larger than the detector resolution, the upper limits for the single resonance X_b apply to the $\Upsilon(1^3D_2)$ as well. The limit on R can be read from Fig.2 for the $\Upsilon(1^3D_2)$ mass, and combined with the measured $\Upsilon(1^3D_2) \to \pi^+\pi^-\Upsilon(1S)$ branching fraction [10], an upper limit on the ratio of cross-sections $\sigma(\Upsilon(1^3D_2))/\sigma(\Upsilon(2S)) < 0.55$ was set. The signal model for $\Upsilon(10860)$ and $\Upsilon(11020)$ is the same as for the X_b but the fitting range was extended and the background polynomial order was extended to three. No evidence for $\Upsilon(10860)$ and $\Upsilon(11020)$ was found either.

3. Conclusions

The $X(3872)$ is the best-studied of the new hidden-charm states seen in the last decade. It is observed at the LHC and the ratio $R = [\sigma(pp \to X(3872))B(X(3872) \to \pi^+\pi^- J/\psi)]/[\sigma(pp \to \psi(2S))B(\psi(2S) \to \pi^+\pi^- J/\psi)]$ is measured to be $(6.56 \pm 0.29 \pm 0.65)\%$ [5].

Heavy-quark symmetry suggests the existence of a hidden-beauty partner referred to as X_b, and the search conducted by ATLAS was presented here [9]. No evidence for new narrow states was found for masses in the ranges 10.05-10.31 and 10.40-11.00 GeV. Thus, 95% CL_S upper limits on the ratio R of the X_b production rate to $\pi^+\pi^-\Upsilon(1S)$ compared to the $\Upsilon(2S)$ production rate to the same channel were set, depending on the X_b mass.

A search for the triplet states $\Upsilon(1^3D_J)$ and for the broad $\Upsilon(10860)$ and $\Upsilon(11020)$ states was also performed, with no evidence for signal. For the $\Upsilon(1^3D_2)$ state, the 95% CL_S upper limit for its production in LHC was set to $\sigma(\Upsilon(1^3D_2))/\sigma(\Upsilon(2S)) < 0.55$.

ACKNOWLEDGMENTS

Participation in the conference was partly supported by the European Commission, call: FP7-PEOPLE-2012-IAPP, Grant No: 324318.

References

[1] ATLAS Collaboration, *The ATLAS Experiment at the CERN Large Hadron Collider*, *JINST* **3** (2008) S08003

[2] S.-K. Choi, et al., Belle Collaboration, *Observation of a narrow charmoniumlike state in exclusive* $B^\pm \to K^\pm X(\to \pi^+\pi^- J/\psi)$ *decays*, *Phys. Rev. Lett* **91** (2003) 262001 [hep-ex/0309032v2].

[3] D. Acosta, et al., CDF Collaboration, *Observation of the narrow state* $X(3872) \to J/\psi\pi^+\pi^-$ *in* pp *collisions at* $\sqrt{s} = 1.96$ *TeV*, *Phys. Rev. Lett.* **93** (2004) 072001, [hep-ex/0312021].

[4] V. Abazov, et al., D0 Collaboration, *Observation and properties of the* $X(3872)$ *decaying to* $J/\psi\pi^+\pi^-$ *in* pp *collisions at* $\sqrt{s} = 1.96$ *TeV*, *Phys. Rev. Lett.* **93** (2004) 162002, [hep-ex/0405004].

[5] CMS Collaboration, *Measurement of the* $X(3872)$ *production cross section via decays to* $J/\psi\pi^+\pi^-$ *in pp collisions at sqrts* $= 7$ *TeV*, *J. High Energy Phys.* **1304** (2013) 154, [hep-ex/1302.3968].

[6] ATLAS Collbaboation, *Measurement of the production cross-section of* $\psi(2S) \to J/\psi(\to \mu^+\mu^-)\pi^+\pi^-$ *in pp collisions at* $\sqrt{s} = 7$ *TeV at ATLAS*, *J. High Energ. Phys.* **2014** (2014) 79, [hep-ex/1407.5532].

[7] LHCb Collaboration, *Quantum numbers of the X(3872) state and orbital angular momentum in its* $\rho^0 J\psi$ *decay*, *Phys. Rev.* **D 92**, 011102 (2015), [hep-ex/1504.06339].

[8] LHCb Collaboration, *Evidence for the decay* $X(3872) \to \psi(2S)\gamma$, *Nucl.Phys.* **B 886** (2014) 665-680, [hep-ex/1404.0275]

[9] ATLAS Collbaboation, *Search for the* X_b *and other hidden-beauty states in the* $\pi^+\pi^-\Upsilon(1S)$ *channel at ATLAS*, *Phys. Lett.* **B 740** (2015) 199-217, [hep-ex/1410.4409]

[10] J. Beringer, et al., Particle Data Group, *Review of particle physics*, *Phys. Rev.* **D 86** (2012) 010001 [http://dx.doi.org/10.1103/PhysRevD.86.010001]

[11] G. Cowan, K. Cranmer, E. Gross, and O. Vitells, *Asymptotic formulae for likelihood-based tests of new physics*, *Eur. Phys. J.* **C 71** (2011) 1554, [Erratum: *Eur. Phys. J.* **C 73** (2013) 2501]. [physics.data-an/1007.1727].

[12] ATLAS Collaboration, *Measurement of the differential cross-sections of inclusive, prompt and non-prompt J/ψ production in proton-proton collisions at $\sqrt{s} = 7$ TeV*, *Nucl. Phys.* **B 850** (2011) 387-444 [hep-ex/1104.3038].